Earth Fault Location based on a Modified Takagi Method for MV Distribution Networks

Le Trung Dung, Marc Petit

Earth Fault Location based on a Modified Takagi Method for MV Distribution Networks

T.D. LE [(1)], M. PETIT [(1)]
[(1)] Geeps, CNRS UMR 8507
CentraleSupélec, UPSud and UPMC
Gif-sur-Yvette, France
Trungdung.le@centralesupelec.fr

***Abstract*—In this paper, an earth fault location algorithm is developed for distribution networks with resistance-earthed neutral. The algorithm is actually a modified version of Takagi method which was initially applied for HV transmission lines. In the proposed algorithm, fault location is performed by means of a searching process on each homogeneous section of MV lines. The voltage and current information at the beginning of each section, which are needed for the process, will be estimated from measurements at the substation and the network parameters. To improve the accuracy, capacitances of underground cables are also taken into account in the fault distance formula. The simulation results on a CIGRE benchmark network are very encouraging, even with impact of distribution load uncertainty.**

***Index Terms*—Distribution Networks; Earth Fault Location; Modified Takagi Algorithm**

I. Introduction

Fault location in distribution networks has been an interesting research topic for many years, for which different proposed methods could be classified in two main categories [1]-[2]: standard techniques (phasor-based algorithms), and non-standard techniques (transient-based, DMS-based and Artificial-Intelligent-based algorithms). The former, which work directly with fundamental frequency currents and voltages, don't require expensive measuring devices with a high sampling rate. However, high precision could hardly be reached with these algorithms due to some particularities of the distribution networks: unbalance, heterogeneity of feeder lines, lateral branches, tapped loads and shunt capacitance of underground cables [3].

One of well-known phasor-based algorithms is the Takagi method [4]-[5], which was initially developed for transmission networks. The key idea is to compensate the impact of fault resistance by means of a polarizing quantity that is in phase with earth fault current. In the original version, the superposition fault current (difference between fault and pre-fault current) was used as polarizing quantity. In a recent research [6], the authors made an attempt to adapt the Takagi algorithm into distribution networks by using an estimate of fault current as polarizing quantity. This estimate was calculated as the sum of the measured neutral current at the substation and the total residual capacitive currents of the entire network. The latter could be determined from the measured residual voltage, also at the substation, and by making the cross-multiplication with the reference values: maximum of residual voltage and maximum of total capacitive current during a bolted single line-to-ground fault. Despite of improvements compared to the original Takagi algorithm, distance errors still exist and increase with fault resistance. This problem is linked with the phase angle error in fault current estimation.

In this study, an improved version of fault current estimation is proposed. For a better accuracy, the total capacitive current of the network will be split into two parts: one of sound feeders will be measured by the feeder relays; one of faulty feeder will be calculated thanks to the zero-sequence voltages along this feeder. Details about the calculation will be shown in the next section, along with the modification of the Takagi formula to take into account the line capacitance between substation and fault. The section III presents the searching process to deal with heterogeneous feeder lines and others particularities of MV distribution grids. Performance tests will be carried out with a CIGRE benchmark MV network [7] in the section IV. Finally, conclusions and perspectives will be given in section V.

II. Modifiied Takagi Method for Homogeneous MV Feeder

A. Consideration of line capacitance

In this section, earth fault is assumed to be on a homogeneous feeder and on phase *a*. Fig. 1 shows the positive sequence impedance of line section from protection to fault. The PI model is used for taking into consideration of line capacitance. The Kirchhoff's Voltage Law (KVL)

978-1-4673-8463-6/16/$31.00

equation can be written as in (1) for positive sequence network:

$$V_{1B} = Z_1 * (I_1 - I_{1capa}) + V_{1F} = x * z_1 * (I_1 - j\omega/2 * x * c_1 * V_1) + V_{1F} \qquad (1)$$

In the same manner, KVL equations are also written for negative and zero sequence networks:

$$V_{2B} = Z_2 * (I_2 - I_{2capa}) + V_{2F} = x * z_2 * (I_2 - j\omega/2 * x * c_2 * V_2) + V_{2F} \qquad (2)$$

$$V_{0B} = Z_0 * (I_0 - I_{0capa}) + V_{0F} = x * z_0 * (I_0 - j\omega/2 * x * c_0 * V_0) + V_{0F} \qquad (3)$$

At the fault point *F*:

$$V_{aF} = R_F * I_F \qquad (4)$$

In these equations:

Indices *1*, *2*, *0*: for positive, negative and zero sequence networks respectively

x: distance to fault (km)

Z, *z*: impedance (Ω) and per unit length impedance (Ω/km) of line section from protection to fault

C, *c*: capacitance (Ω) and per unit length capacitance between protection and fault (Ω/km)

$\omega = 2\pi f$ with $f = 50$ Hz

By summing (1), (2), (3) and by taking into account (4), the following relation can be obtained:

$$V_{aB} = x * z_1 * (I_a + K * I_0) - j * 0.5 * \omega * x^2 * z_1 * c_1 * (V_{aB} + K_c * V_0) + R_F * I_F \qquad (5)$$

where $K = (z_0 - z_1)/z_1$ and $K_c = (z_0 c_0 - z_1 c_1)/(z_1 c_1)$

V_{aB} is the voltage of phase *a* at node *B*

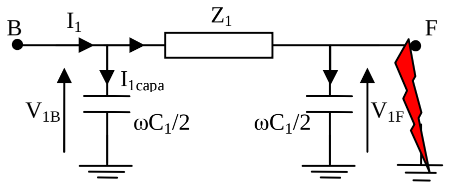

Figure 1. PI model of line section from protection to fault – Positive sequence network

If a current I_{pol} that is in phase with the fault current I_F could be determined, then multiply two sides of (5) with I_{pol}, and take only the imaginary part of the new relation. The result of this transformation is a quadratic equation from which the distance to the fault *x* can be estimated:

$$mx^2 + nx + p = 0 \qquad (6)$$

where $m = \text{Im}\{j * 0.5 * \omega * z_1 * c_1 * (V_{aB} + K_c * V_0) * I_{pol}^*\}$

$n = \text{Im}\{-z_1 * (I_a + K * I_0) * I_{pol}^*\}$

$p = \text{Im}\{V_{aB} * I_{pol}^*\}$

In this paper, an estimate of fault current I_{fest} is chosen to define the polarizing quantity ($I_{pol} = I_{fest}$).

B. *Estimation of fault current I_{fest}*

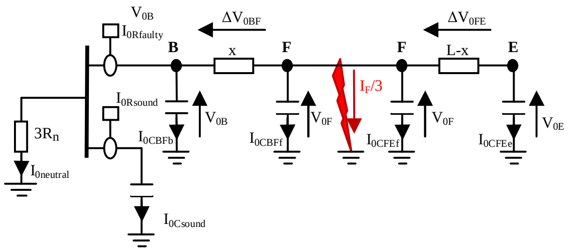

Figure 2. Generic zero-sequence network of MV distribution grids

Fig. 2 shows a generic zero sequence network of a MV distribution grid with resistive grounding (R_n). On the faulty feeder, two PI models represents two feeder sections upstream (*BF*) and downstream (*FE*) with respect to the fault point *F*. Impact of the rest of the grid is modeled by aggregating the zero capacitance of all sound feeders. I_{fest} will be determined as follows:

$$I_{fest} = -3 * \left(I_{0neutral} + I_{0Csound} + \sum_{K,l} I_{0CKl} \right) \qquad (7)$$

where $I_{0neutral}$ is the zero neutral current

$I_{0Csound}$ is the total zero capacitive current of sound feeders

I_{0CKl} is the zero capacitive current of the K^{th} section at node *l*

$I_{0neutral}$ and $I_{0Csound}$ can be measured by current sensors at the substation, while I_{0CKl} will be estimated from zero voltage V_{0l} ($I_{0CKl} = j*0.5*\omega*C_{0K}*V_{0l}$). In fact, there is only voltage at busbar that is measured. Voltage information at others nodes will be determined from busbar voltage and the voltage drop between busbar and the node in question. In this case, voltage at the fault point *F* is calculated as in (8):

$$V_{0F} = V_{0B} - (I_{0B} - I_{0capaBFb}) * z_0 * x \qquad (8)$$

As can be seen in (8), the distance *x* needs to be known to determine V_{0F}, but *x* is our unknown. A solution is to begin the process by assuming a value of fault distance x_{sup}, from which the zero sequence voltages, as well as the total capacitive residual current of the faulty feeder can be evaluated. The next step is to calculate I_{fest} from (7) and finally the estimated distance x_{est} from (6). Compare x_{sup} and x_{est}, theoretically if x_{sup} is equal to the real fault distance x_{real}, then x_{est} will be also equal to x_{real} or in other words, the equility $x_{sup} = x_{est}$ should be verified. If it is not the case, x_{sup} should be varied until the real fault distance is determined. In general, x_{sup} will be varied from 0 to the length *L* of the faulty feeder *BE*. The procedure is resumed in the flowchart of Fig.3. In fact, the increment of x_{sup} is discrete, so the difference $\Delta x = |x_{est} - x_{sup}|$ will unlikely be zero. Therefore, the chosen estimate of fault distance *d* is taken from one corresponding to the minimum of Δx.

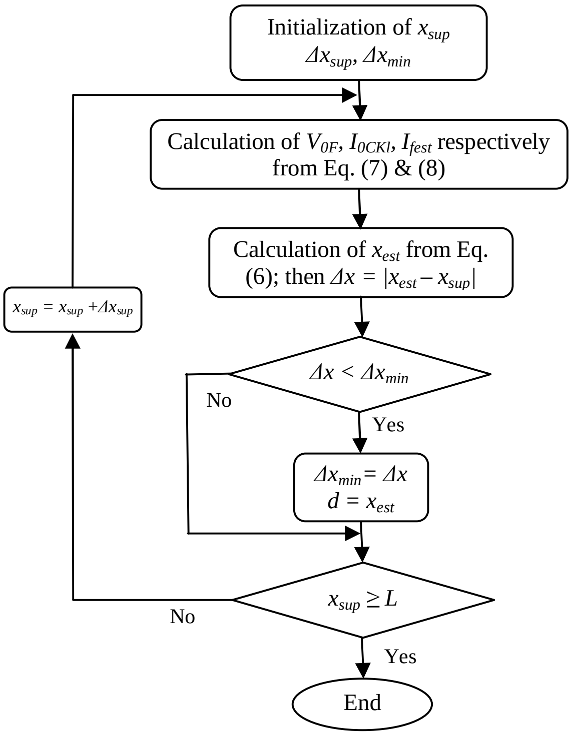

Figure 3. Fault location algorithm on homogeneous feeder

III. ALGORITHM FOR HETEROGENEOUS MV FEEDER

As previously mentioned, MV feeders are indeed heterogeneous, consisting of a number of homogeneous sections. However, the Modified Takagi method could only be applied on homogeneous feeder. As a result, the fault location process should be performed successively on each section.

The process starts with the first section, at the beginning of the feeder. For this section, voltage and current sensors located in the substation are available. The procedure of Fig.3 is carried out and an estimate *d* of the fault distance is recorded. Then the process continues with the immediate downstream section. The initial value of Δx_{min} for this second section is taken from the outcome of the searching process on the previous section. As in the current section, there is no sensor, voltage and current informations should be estimated from ones from the first section. However, the grid is three-phase system with effects of mutual inductance and capacitance. For simplicity, the estimation, which is based on the two Kirchhoff's law in theory of circuit, will be performed on sequence networks. The phase voltages and currents will be reproduced from the sequence quantities. To take into account the impact of distribution loads, each of them is modeled by its equivalent impedance at rated conditions or if possible, one given from the statistical data. This searching process will be continued until the last section of the feeder in question.

It should be noted that MV feeders may contain lateral lines. Consequently, there may be several possible paths from substation to remote ends of the feeder. A remote end is the node from which there is no downstream line. To handle this point, the fault location process will search on each possible path. Furthermore, when searching on a given path, the lateral lines with respect to this path will be reduced to equivalent impedances at the bifurcation, as shown in Fig. 4 for the sake of example. Hence the estimation of voltage and current measurements during the searching process can be done identically as in case of no lateral lines. For each path, the fault location will be the one where Δx_{min} reaches its minimum, for all searched sections. This means that there can be multiple solutions in fault location, as reported in some previous papers [8]-[9]. To eliminate some apparently unacceptable solutions, an upper limit of 0.1 km is set for Δx_{min} in this paper. In other words, a found fault location that corresponds to Δx_{min} bigger than 0.1 km will not be considered for final results.

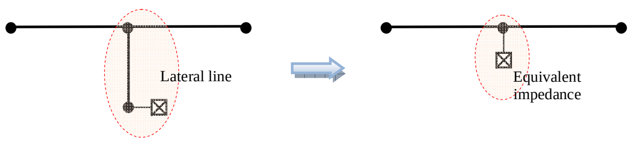

Figure 4. Estimation of measurements in case of lateral lines

IV. TEST NETWORK AND RESULTS

The single line diagram of the CIGRE benchmark MV (20 kV) grid [7], which is used for performance test, is shown in Fig. 5. There are two "mixed" radial feeders:

- Feeder 1: with bifurcation, composed of 2.82 km of overhead lines and 11.84 km of underground cables, 5.7 MVA of total loads
- Feeder 2 : no bifurcation, composed of 7.88 km of overhead lines and 0.32 km of underground cables, 1.2 MVA of total loads

For two feeders, the shortest section length is 0.32 km (sections 0-1, 8-9 and 0-12). The longest one is 4.89 km (section 12-13). Details of grid parameters are given in Appendix.

Grid faults are simulated with this test network with focus on the feeder 1 because of its lateral lines: on each section of the feeder, three positions of earth fault will be chosen to simulate: at 10%, 50% and 90% of the section length. For each position, the fault resistance R_F will be varied from 0 to 1000 Ω (7 values of R_F: 0, 10, 50, 100, 200, 500, 1000 Ω). As the feeder 1 is composed of 11 sections, there are totally 231 simulations that will be performed with Simulink/SimPowerSystems. As mentioned previously, voltages at busbar and currents at the beginning of each feeder and on the neutral grounding are "measured".

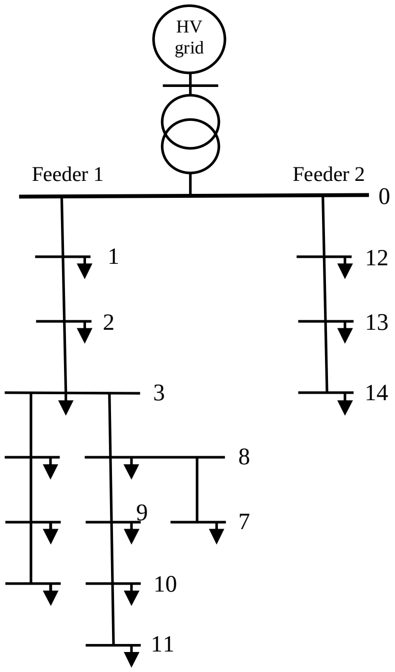

Figure 5. CIGRE benchmark MV network

A. No uncertainty in load consumptions

In this subsection, load consumptions are supposed to be known for fault location and equal to ones given in Appendix. By applying the proposed fault location algorithm, estimates of fault distance d are determined for each simulation. Respectively, Tables I & II show results for two following fault cases:

- Fault n°9 at 90% of the length of Section 2-3, with $R_F = 200\ \Omega$
- Fault n°28 at 10% of the length of Section 10-11, with $R_F = 200\ \Omega$

The status "OK" will be indicated in case that the found section is the real faulty one or it is one of adjacent sections of the real one [6].

TABLE I. FAULT LOCATION RESULTS FOR FAULT N°9 ($R_F = 200\ \Omega$)

Found section	Found distance (m)	Distance error (m)	Distance error (%)	Status
2-3	7070	48	0.46	OK

TABLE II. FAULT LOCATION RESULTS FOR FAULT N°28 ($R_F = 200\ \Omega$)

Found section	Found distance (m)	Distance error (m)	Distance error (%)	Status
5-6	9980	NA	NA	Not OK
8-7	10010	NA	NA	Not OK
9-10	9920	63	0.61	OK

As can be seen in Table I, for the first case, the proposed algorithm gives the unique solution that is on the real faulty section (between nodes 2&3). The absolute error with respect to the real fault location is about 48 m. The relative error is 0.46%, which is calculated as the ratio between absolute error and the length of the feeder:

$$\textit{Dist. error (\%)} = \textit{Dist. error (m)/Feeder length (m)*100} \qquad (9)$$

On the other hand, for the second case, the algorithm gives three solutions (Table II) but none of them is on the real faulty section (between nodes 10&11). In fact, the section 10-11 is on a lateral line, which leads to the multiple solutions in fault location. Three found fault locations correspond to three possible paths from substation to remote ends of the feeder. In particular, the third solution gives the fault location on an adjacent section (between nodes 10&11) of the real faulty one. This is mainly because of calculation errors and the fact that the real fault is located at the beginning of a short section (at 10% of a 330 meter section line). Furthermore, the real fault distance is 9983 m from the substation. The found distances are pretty close to this figure. The absolute and relative errors are also calculated for the found section with the "OK" status and given in Table II.

Table III and Fig. 6 illustrate the performances of our algorithm for all 231 simulations.

In Table III, the accuracy in the identification of faulty section is shown. In the first line of results, the identification will be considered as correct if it indicates exactly the real faulty section. In the second line, a correct identification may indicate either the real faulty section or adjacent ones. As can be seen in this table, for the first approach of evaluation, the accuracy starts to decrease rapidly from $R_F = 200\ \Omega$ and drops to 60.61% corresponding to $R_F = 1000\ \Omega$. As demonstrated for the fault case of Table II, wrong identifications happen when faults are at the extremities of short sections. In contrast, for the second approach when the adjacent sections are considered, the accuracy of the proposed algorithm remains high even with high impedance faults (96.97% correct identifications corresponding to $R_F = 1000\ \Omega$).

Fig. 6 shows the evolution of mean relative error and the corresponding standard deviation in fault distance estimation with respect to fault resistance. The calculation is performed for all fault location results with the "OK" status. It can be seen that the mean error increases with the fault resistance but remains low. It reaches the maximal value of 1.95% for $R_F = 1000\ \Omega$.

TABLE III. ACCURACY IN FAULTY SECTION IDENTIFICATION (%)

R_F (Ω)	0	10	50	100	200	500	1000
faulty section only	100	100	100	100	90.91	69.7	60.61
faulty& adjacent sections	100	100	100	100	100	96.97	96.97

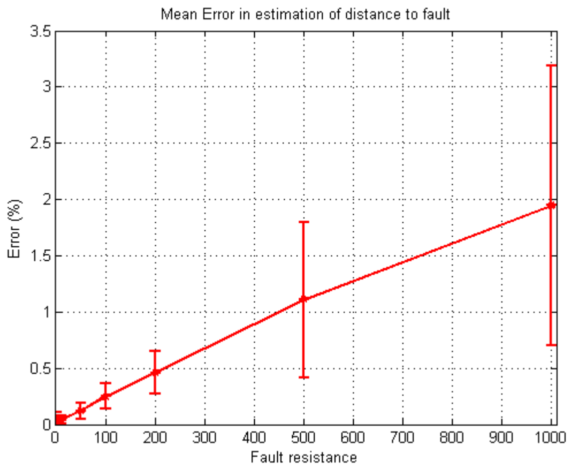

Figure 6. Relative error in fault distance estimation

B. *Impact of uncertainty in load consumptions*

The fault location in previous paragraph was performed, assuming that load consumptions are perfectly known. In fact, it is rarely the case in distribution networks where only the statistical data about loads are generally known. Hence it is necessary to study the impact of uncertainty of load data on performances of the proposed algorithms.

In this subsection, analysis is performed for R_F = 200 Ω. The fault location algorithm is run 200 times on each of 33 fault positions. On each time that the algorithm is performed, load consumptions are varied according to the Gaussian distribution in which mean values of loads are the ones indicated in Appendix and standard deviations { σ } are 16.67% of the corresponding mean values (i.e. the three standard deviation 3σ will be 50% of mean values).

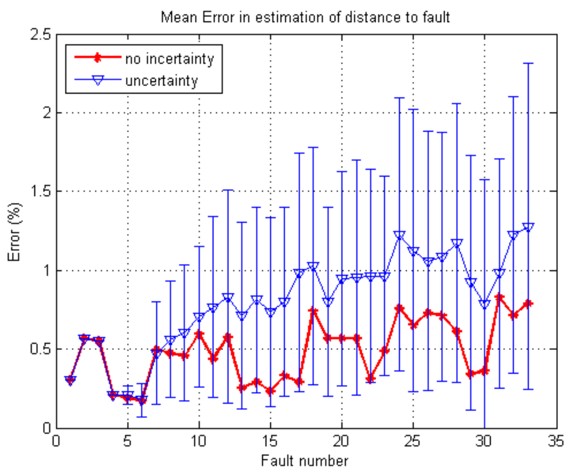

Figure 7. Relative error in fault distance estimation – Impact of load uncertainty

Results show that the accuracy in faulty section identification remains high:

- 96.2% of identifications indicate the real faulty section.
- 99.7% of identifications indicate the real faulty section or one of adjacent sections.

Fig. 7 shows mean errors in fault distance estimation for 33 fault positions on Feeder 1 in case of no uncertainty on load consumptions (red plot) and in case of uncertainty (blue plot). In the latter, error bars related to confidence interval of standard deviation are also added. It should be noted that for some fault positions at the first sections of Feeder 1 (which correspond to faults from n°1 to n°6), the mean errors in case of uncertainty are nearly the same as ones in case of no uncertainty. For the others, mean errors are higher than one without uncertainty. In fact, load uncertainty will principally impact on measurement estimation (voltages, currents) during the section-by-section searching process. The more the process goes to the remote sections, the more the uncertainty will impact the results of fault location. Furthermore, the higher the load consumption is, the more its uncertainty will change the results. The highest mean error is 1.28% for fault n°33 (at 90% of the length of section 8-7).

V. CONCLUSIONS

In this paper, a novel Modified Takagi Method is proposed for fault location in distribution networks with resistive grounding. The estimation of fault current is performed meticulously to find the polarizing quantity. Moreover, the Takagi formula is revised to take into account the capacitance of underground cables. The fault location algorithm is carried out on each homogeneous section of the faulty feeder.

Performance tests are also performed on a CIGRE benchmark network. Results show that the algorithm is able to indicate, for almost cases, the real faulty section or adjacent ones, even with high impedance fault (R_F = 1000 Ω). In addition, the relative error in fault distance estimation is small (1.95% of feeder length with R_F = 1000 Ω). A sensitivity analysis is carried out for impact of load uncertainty with R_F = 200 Ω. The proposed algorithm can still give good performances. Mean errors increase but remain small (maximal value of 1.28%).

In the future works, the impact of distributed generators connected to the MV networks will be examined. Furthermore, the problem of multiple solutions will be addressed in order to find the unique real faulty section.

REFERENCES

[1] M.M. Saha, J.J. Izykowski, E. Rosolowski, *Fault Location on Power Networks*, Springer, 2010.

[2] *IEEE Guide for Determining Fault Location on AC Transmission and Distribution Lines*, IEEE Std C37.114, 2004.

[3] J. Mora-Florez, J. Meléndezal, and G. Carrillo-Caicedo, "Comparison of impedance based fault location methods for power distribution systems," *Electr. Power Syst. Res.*, vol. 78 (4), pp. 657–666, 2008.

[4] T. Takagi, Y. Yamakoshi, M. Yamaura, R. Kondow, and T. Matsushima, "Development of a New Type Fault Locator Using the One-Terminal Voltage and Current Data," *IEEE Trans. on Power Apparatus and Systems*, Vol. PAS-101, No. 8, August 1982.

[5] K. Zimmerman and D. Costello, "Impedance-based fault location experience," in *Proc. of 58th Annual Conference for Protective Relay Engineers (2005)*, pp. 211–226
[6] R. Marguet, "Improved Fault Localization Method for Electrical Power Distribution Networks," PhD Dissertation, Univ. de Grenoble, 2015.
[7] P. Janssen, "Monitoring, protection and fault location in power distribution networks using system-wide measurements", PhD Dissertation, Univ. Libre de Bruxelles, 2014.
[8] G. Morales-España and J. Mora-Flórez, "Elimination of Multiple Estimation for Fault Location in Radial Power Systems by Using Fundamental Single-End Measurements," *IEEE Trans. on Pow. Del.*, vol. 24, no. 3, pp. 1382 – 1389, Jul. 2009.
[9] R. Dashti and J. Sadeh, "Fault section estimation in power distribution network using impedance-based fault distance calculation and frequency spectrum analysis," *IET Gener. Transm. Distrib.*, vol. 8, iss. 8, pp. 1406–1417, 2014.

APPENDIX

Test network characteristics:

- HV network: 63 kV, P_{cc} = 600 MVA, X/R = 10
- HV/MV Transformer: 63/20 kV, S_{rated}= 36 MVA, u_{cc} =12%
- Neutral impedance: R_n=80 Ω (resistive grounding).
- Line characteristics & load data:

Fbus	Tbus	Length (km)	r_1 (Ω/km)	x_1 (Ω/km)	r_0 (Ω/km)	x_0 (Ω/km)	c_1 & c_0 (μF/km)	Load (MVA) at Tbus
0	1	0.32	0.34	0.13	1.02	0.52	0.32	0.54
1	2	2.82	0.58	0.37	0.77	1.1	0.02	0.54
2	3	4.42	0.16	0.11	0.49	0.45	0.32	0.54
3	4	0.61	0.26	0.12	0.79	0.48	0.32	0.45
4	5	0.56	0.35	0.13	1.06	0.52	0.32	0.75
5	6	1.54	0.34	0.13	1.01	0.5	0.32	0.57
3	8	1.3	0.17	0.12	0.52	0.46	0.32	0.61
8	9	0.32	0.34	0.13	1.02	0.52	0.32	0.68
9	10	0.77	0.4	0.13	1.2	0.53	0.32	0.57
10	11	0.33	0.37	0.13	1.1	0.53	0.32	0.34
8	7	1.67	0.29	0.12	0.88	0.49	0.32	0.09
0	12	0.32	0.34	0.13	1.02	0.52	0.32	0.54
12	13	4.89	0.34	0.36	0.45	1.07	0.02	0.04
13	14	2.99	0.2	0.12	0.27	0.37	0.02	0.60